

**Report on Bioinformatics Summer Research Internship at Manna Biotech  
May 10 2025 - June 26 2025**

Project Title

**Inhibition of the PTEN Gene as a Strategy for Enhancing Central  
Nervous System (CNS) Regeneration and Functional Recovery  
&  
Identification of Hub Genes in Ankylosing Spondylitis Through  
GEO Dataset Analysis and Protein Interaction Docking**

A detailed report of summer internship  
Submitted by

**Dandem Eswar Sai Surya Prasad  
23BTB0A26  
de23btb0a26@student.nitw.ac.in**

Under the esteemed guidance and supervision of

**Dr. Manne Munikumar  
Director – Academics & Trainings  
Manna Biotech, Hyderabad**

# CONTENTS

Acknowledgement	05
-----------------	----

Abstract	06
----------	----

## CHAPTER 01

1.1 Introduction	07
------------------	----

1.2 Literature review	07
-----------------------	----

1.3 Materials and Methods	09
---------------------------	----

1.3.1 Retrieval of PTEN amino acid sequence and structure

1.3.2 Structural validation

1.3.3 Active site identification

1.3.4 Sequence homology and phylogenetic analysis

1.3.5 Ligand selection

1.3.6 Molecular docking

1.4 Results and Discussions	13
-----------------------------	----

1.4.1 Structure validation of PTEN (PDB ID: 5BUG)

1.4.2 Active site identification

1.4.3 Docking results

1.4.4 Graphical Abstract

1.4.5 Comparison with literature

1.5 Conclusion	18
----------------	----

1.6 References	19
----------------	----

## **CHAPTER 02**

<b>2.1 Introduction</b>	<b>20</b>
<b>2.2 Literature review</b>	<b>21</b>
<b>2.3 Materials and Methods</b>	<b>22</b>
2.3.1 Dataset Selection	
2.3.2 Differential Gene Expression Analysis	
2.3.3 Pathway and Functional Enrichment	
2.3.4 Protein Interaction Network and Hub Gene Identification	
2.3.5 Protein Structure Modelling	
2.3.6 Protein-Protein Docking	
2.3.7 Protein-Epitope Docking	
2.3.8 Summary	
<b>2.4 Results and Discussions</b>	<b>24</b>
2.4.1 Differential Expression and Pathway Enrichment	
2.4.2 PPI Network and Hub Gene Identification	
2.4.3 Protein-Protein Docking	
2.4.4 Protein-Epitope Docking	
2.4.5 Graphical Abstract	
<b>2.5 Conclusion</b>	<b>28</b>
<b>2.6 References</b>	<b>30</b>

## List of Figures

<i>Fig. 1.3.1. PTEN 3D structure (PDB ID: 5BUG)</i>	09
<i>Fig. 1.4.1.A. PROSA Result</i>	13
<i>Fig. 1.4.1.B. UCLA Saves Ramachandran Plot analysis</i>	13
<i>Fig. 1.4.1.C. Theoretical Energy Data</i>	14
<i>Fig. 1.4.2. Active Site Residues</i>	15
<i>Fig. 1.4.3.A. 3D Docked Complex</i>	15
<i>1.4.3.B. 2D Interacting Residues</i>	16
<i>Fig. 2.4.1.A</i>	24
<i>Fig. 2.4.1.B. Oxidative Phosphorylation pathway from ShinyGO</i>	24
<i>Fig. 2.4.2. Cluster 1 from MCODE</i>	25
<i>Fig. 2.4.3.A COX5B Swiss-Model</i>	25
<i>Fig. 2.4.3.B. Complex</i>	25
<i>Fig. 2.4.4.A epitope Model by PEP-FOLD3</i>	26
<i>Fig. 2.4.4.B. COX5B and Epitope docked complex</i>	26

## List of Tables

<i>Table 1.4.1. Structural Validation Data</i>	14
<i>Table 1.4.3. Comparison of binding scores of known ligands</i>	16
<i>Table 2.4.2. Hub gene clusters from MCODE</i>	25
<i>Table 2.4.3. Top 10 docking solution data</i>	26

## Acknowledgment

I would like to take this opportunity to express my heartfelt gratitude and deep appreciation to **Dr. Manne Munikumar**, Director – Academics & Trainings Manna Biotech, my esteemed guide and mentor, for his invaluable guidance, unwavering patience, and consistent encouragement throughout the course of this internship. Over the past 45 days, under his expert supervision, I have not only learned but truly discovered the researcher within myself. Dr. Munikumar introduced me to a wide range of bioinformatics tools and techniques, many of which were entirely new to me at the outset. Through his methodical teaching style, insightful suggestions, and constant motivation, I was able to build confidence in handling complex datasets, analysing gene expression profiles, and interpreting results with scientific rigor. His ability to simplify intricate concepts, coupled with his readiness to clarify doubts at every stage, played a pivotal role in shaping the direction and quality of my work.

Throughout this internship, Dr. Munikumar fostered an environment of curiosity and independent thinking. He encouraged me to critically analyse the results, refine methodologies, and explore new avenues wherever possible. The sessions on GEO datasets, Cytoscape analysis, and docking studies were particularly transformative, as they enabled me to grasp not only the technical skills but also the biological significance behind each step. The knowledge, discipline, and research ethics I have imbibed under his mentorship will undoubtedly guide me in all my future scientific endeavours.

I am also deeply thankful to **Dr. Chathyusha K B**, MD & CEO Manna Biotech, for her unwavering moral support and inspirational leadership. Her enthusiasm for innovation and excellence, combined with her approachable and supportive nature, created an atmosphere where I felt both valued and motivated. Her encouraging words and constant belief in the potential of young researchers like me have greatly contributed to my confidence and determination to excel in this field. The positive work environment she fosters has been instrumental in making this internship a truly enriching experience.

## Abstract

### **Inhibition of the PTEN Gene as a Strategy for Enhancing Central Nervous System (CNS) Regeneration and Functional Recovery**

The phosphatase and tensin homolog (PTEN) gene have been widely studied for its role in inhibiting neural regeneration, and its inhibition presents a promising strategy for enhancing central nervous system (CNS) recovery. In this project, we conducted an extensive structural and functional analysis of PTEN, with a focus on its potential inhibition. The 3D structure of PTEN (PDB ID: 5BUG) was analysed using tools such as PROQ, PROSA, and SAVES by UCLA to evaluate its structural integrity and reliability through Ramachandran plot assessments. Active sites within the PTEN structure were visualized using Discovery Studio, aiding in the identification of key binding pockets. Subsequently, we performed BLAST searches and multiple sequence alignments (MSA) with orthologous proteins from different organisms to assess evolutionary conservation. Phylogenetic trees were constructed using ClustalW and MEGA, providing insights into PTEN's evolutionary relationships. Building upon these findings and guided by literature evidence, we carried out molecular docking studies. Among the tested ligands, **2,2,2-Trifluoro-N-(4-methoxy-phenyl)-acetamide** was identified as a promising inhibitor, showing strong binding affinity to PTEN's active site, thereby supporting its potential for promoting CNS regeneration.

### **Identification of Hub Genes in Ankylosing Spondylitis Through GEO Dataset Analysis and Protein Interaction Docking**

In the second phase of this research, we focused on Ankylosing Spondylitis (AS), aiming to identify key hub genes and interaction targets through integrated bioinformatics approaches. We utilized gene expression profiles from NCBI GEO dataset GSE25101, performing differential gene expression analysis via GEO2R to identify significant upregulated and downregulated genes (DEGs). The DEGs were systematically filtered and categorized using Excel-based tools. Further, metabolic and functional pathway enrichment was conducted through ShinyGO, enabling us to map the DEGs to biologically relevant pathways. Using the significantly enriched genes, we constructed protein-protein interaction (PPI) networks in STRING and visualized them in Cytoscape. The MCODE plugin facilitated clustering within the PPI network, leading to the identification of two major hub gene clusters that are potentially critical in the pathogenesis of Ankylosing Spondylitis. We propose to extend this work by performing protein-protein docking and protein-epitope docking of these hub proteins using Hex software, to further validate their interaction patterns and therapeutic relevance. These combined approaches aim to deepen our understanding of AS molecular mechanisms and identify novel targets for therapeutic interventions.

## CHAPTER 1

# **Inhibition of the PTEN Gene as a Strategy for Enhancing Central Nervous System (CNS) Regeneration and Functional Recovery**

---

### **1.1 Introduction**

The phosphatase and tensin homolog (PTEN) gene encode a tumour suppressor protein that negatively regulates the PI3K/AKT signalling pathway, thereby controlling cell growth, survival, and proliferation. In the context of the central nervous system (CNS), PTEN plays a critical role in inhibiting axonal regeneration following injury. Its activity limits the intrinsic capacity of neurons to regrow damaged axons, making it a key molecular barrier in CNS recovery. Recent studies suggest that targeted inhibition of PTEN could promote neuroregeneration and functional recovery after spinal cord injuries or neurodegenerative conditions.

This project aims to analyse the structure and evolutionary conservation of PTEN, identify its functional domains, and explore potential inhibitors through molecular docking approaches. By investigating PTEN at both the sequence and structural levels, we sought to identify a promising small molecule that could serve as a PTEN inhibitor, providing a foundation for therapeutic strategies aimed at enhancing CNS regeneration.

### **1.2 Literature review**

Central nervous system (CNS) injuries, including spinal cord trauma, often result in permanent loss of motor and sensory function due to the limited regenerative capacity of neurons. One of the key molecular barriers to axonal regrowth is the activity of the phosphatase and tensin homolog (PTEN), a well-known tumor suppressor gene. PTEN negatively regulates the PI3K/AKT/mTOR signalling pathway, which is essential for cell survival, growth, and regeneration (Park et al., 2008). In the CNS, PTEN activity suppresses intrinsic growth programs, preventing axonal regeneration after injury. As a result, there has been growing interest in exploring PTEN as a therapeutic target to promote neural repair.

Several animal models studies have demonstrated that PTEN deletion or knockdown enhances axonal regeneration and functional recovery following CNS injuries. For example, Liu et al. (2010) showed that conditional knockout of PTEN in adult corticospinal neurons led to robust axonal regrowth and

improved motor function in mice with spinal cord injury. These findings suggest that inhibiting PTEN activity could unlock regenerative pathways that are otherwise dormant in adult neurons. However, while genetic deletion provides valuable mechanistic insights, it is not directly translatable to clinical settings, prompting interest in the discovery of small molecule PTEN inhibitors.

In recent years, bioinformatics and molecular docking approaches have emerged as powerful tools for identifying potential PTEN inhibitors. Computational methods allow for the screening of thousands of compounds, structural validation of PTEN's active sites, and prediction of ligand binding affinities. Structural validation tools like PROQ, PROSA, and Ramachandran plot analysis are commonly employed to ensure that the protein model used for docking is reliable. Furthermore, visualization of active sites using platforms such as Discovery Studio helps in understanding key residues involved in PTEN's phosphatase activity, which is critical for rational drug design (Leslie et al., 2015).

Comparative sequence analysis through BLAST and multiple sequence alignment (MSA) has also contributed to understanding the evolutionary conservation of PTEN across species, emphasizing its fundamental role in cellular processes. Phylogenetic studies highlight that PTEN is highly conserved, reinforcing the importance of targeting regions specific to its phosphatase domain to achieve selective inhibition without off-target effects (Ming et al., 2013).

Despite significant progress, the search for a clinically viable PTEN inhibitor remains ongoing. Molecules like **VO-OHpic** (a vanadate derivative) have shown PTEN inhibitory activity in vitro, but challenges such as specificity, bioavailability, and toxicity persist (Rosivatz et al., 2006). The identification of **2,2,2-Trifluoro-N-(4-methoxy-phenyl)-acetamide** as a potential PTEN inhibitor through molecular docking represents a step toward expanding the repertoire of candidate molecules that could one day translate into CNS regenerative therapies.



## 1.3 Materials and Methods

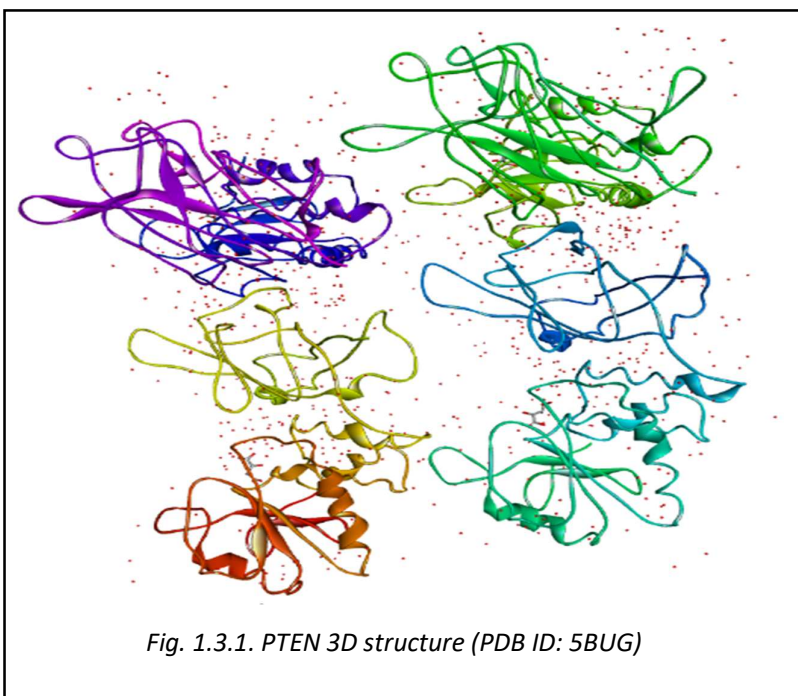
### 1.3.1 Retrieval of PTEN amino acid sequence and structure

Amino Acid sequence is retrieved from Uniprot, with uniprot ID: **P60484**, Fasta format of this sequence is as follows

```
>sp|P60484|PTEN_HUMAN Phosphatidylinositol 3,4,5-trisphosphate 3-phosphatase and  
dual-specificity protein phosphatase PTEN OS=Homo sapiens OX=9606 GN=PTEN PE=1  
SV=1
```

```
MTAIIKEIVSRNKRRYQEDGFDLDTYIYPNIIAMGFPAERLEGVYRNNIDDVVRFLD  
SKHKNHYKIYNLCAERHYDTAKFNCRVAQYPFEDHNPPQLELIKPFCELDLQWLSE  
DDNHVAAIHCKAGKGRTGVMICAYLLHRGKFLKAQEALDFYGEVTRDKKGGVTIPS  
QRRYVYYYSYLLKNHLDYRPVALLFHKMMFETIPMFSGGTCNPQFVVCQLKVKIYS  
SNSGPTRREDKFMFYFEFPQPLPVCGLDIKVEFFHKQNKMLKKDKMFHFWVNTFFIPGP  
EETSEKVENGSLCDQEIDSICSIERADNDKEYLVLTLTKNDLDKANKDKANRYFSPNF  
KVKLYFTKTVEEPSNPEASSSTSVTPDVSDNEPDHYRYSDDTSDPENEPFDEDQHTQ  
ITKV
```

The three-dimensional structure of human PTEN was obtained from the RCSB Protein Data Bank (PDB) to serve as the basis for molecular modelling and docking studies. The selected structure was PDB ID: **5BUG**, which represents the phosphatase domain of PTEN at high resolution. The structure file was downloaded in Legacy PDB format for further validation and docking analysis.



### 1.3.2 Structural validation

To ensure the structural quality of the PTEN model prior to docking, the retrieved PDB file was subjected to validation using multiple tools:

**PROQ** (Protein Quality Predictor) was used to evaluate overall model quality based on predicted LGscore and MaxSub values.

**PROSA-web** was applied to assess the overall energy profile and identify any regions with potential errors in folding.

**UCLA SAVES** server was utilized to generate a Ramachandran plot, providing insight into backbone dihedral angle distributions and confirming proper stereochemistry.

Together, these analyses confirmed the reliability of the protein structure for subsequent docking studies.

### 1.3.3 Active site identification

Identifying active site regions in a protein is very important in the context of molecular docking, hence to identify active site regions of PTEN protein, the structure was loaded into **Discovery Studio Visualizer**. The software was used to examine and understand the phosphate active site pocket, ligand already present in the PDB Structure of 5BUG was used to identify active site amino acids and their positions before going ahead with molecular docking. This enabled us to determine potential binding regions for inhibitor docking in this PTEN structure.

### 1.3.4 Sequence homology and phylogenetic analysis

The amino acid sequence corresponding to the 5BUG PTEN structure was subjected to BLASTp analysis against the NCBI non-redundant (nr) protein database to identify homologous proteins across a wide range of species. Homologous sequences showing high similarity were selected from animals, plants, and microorganisms to provide a comprehensive view of PTEN conservation across kingdoms.

Selected sequences were aligned using ClustalW, and the resulting multiple sequence alignment (MSA) was used to infer phylogenetic relationships. A phylogenetic tree was constructed in MEGA software using the Neighbour-Joining (NJ) method. To assess the reliability of the inferred tree topology, bootstrapping with 1000 replicates was performed. This analysis provided insights into the evolutionary conservation and divergence of PTEN across diverse taxa.

### 1.3.5 Ligand selection

The search for a suitable PTEN inhibitor was guided by both literature evidence and in silico docking pre-screens aimed at identifying molecules with potential to bind selectively and effectively to the PTEN active site. After a comprehensive review of previously reported small molecules targeting PTEN, the compound **2,2,2-Trifluoro-N-(4-methoxy-phenyl)-acetamide** was chosen for detailed docking analysis. This compound was selected based on its structural features, including a trifluoromethyl group known to enhance membrane permeability and metabolic stability, as well as a methoxyphenyl moiety capable of engaging in favorable aromatic and hydrogen bonding interactions. The molecular structure of this compound was retrieved from PubChem (CID available upon request), and converted into formats suitable for docking, including PDB and mol2, using OpenBabel software.

Beyond this lead compound, other small molecules have been reported in the literature as PTEN inhibitors or modulators. Notably, **VO-OHpic** (a vanadium-based derivative) has been widely studied for its PTEN inhibitory effects (Rosivatz et al., 2006). While effective in vitro, VO-OHpic's clinical utility is limited due to concerns about specificity, bioavailability, and systemic toxicity. Similarly, bisperoxovanadium compounds, such as **bpV** (HOpic), have shown PTEN inhibition activity but suffer from similar drawbacks (Leslie & Downes, 2015).

Recent bioinformatics and docking studies have also identified organic small molecules with PTEN inhibitory potential. For instance, anthraquinone derivatives have been proposed as PTEN inhibitors with reduced toxicity profiles (Koul et al., 2018). Additionally, in silico screening by Zhao et al. (2021) highlighted several novel benzothiazole derivatives as promising PTEN-binding candidates with favorable docking scores and predicted ADMET profiles.

The selection of 2,2,2-Trifluoro-N-(4-methoxy-phenyl)-acetamide for this study was based on its structural drug-like properties, the novelty of its use in PTEN inhibition contexts, and preliminary docking results that indicated a promising binding pose and interaction energy. This compound represents an effort to move beyond metal-based inhibitors toward small organic molecules that may offer improved specificity and reduced toxicity in future experimental validation.

The final list of candidate ligands considered during the study included:

2,2,2-Trifluoro-N-(4-methoxy-phenyl)-acetamide (focus of this study)

VO-OHpic (reference inhibitor, included in literature review)

bpV (HOpic) (bisperoxovanadium reference inhibitor)

Anthraquinone derivatives (reported in Koul et al., 2018)

Benzothiazole derivatives (reported in Zhao et al., 2021)

These candidate molecules were subjected to comparative analysis in terms of binding energy, pose within the PTEN active site, and potential for selective inhibition.

### **1.3.6 Molecular docking**

Molecular docking was employed to predict and analyse the binding interaction between PTEN and the selected inhibitor, 2,2,2-Trifluoro-N-(4-methoxy-phenyl)-acetamide. Prior to docking, the PTEN structure (PDB ID: 5BUG) was prepared using Discovery Studio Visualizer. Unnecessary side chains that could interfere with docking were carefully removed, along with all water molecules present in the structure. This step ensured a clean and focused binding site environment for docking simulations.

Two models of PTEN were generated as part of the docking preparation. The first model retained the co-crystallized ligand from the original PDB file, which served as a reference to identify and define the active site region by highlighting interacting amino acid residues. The second model had the ligand removed to allow for docking of the selected compound without bias from the native ligand pose. Both models were imported into **PyRx**, a versatile docking software suite, where further docking preparations were conducted. Using the model with the native ligand, the precise location of the PTEN active site was mapped based on key amino acid residues. This information was used to define the docking grid in PyRx. The model without the native ligand was then used for the actual docking simulation.

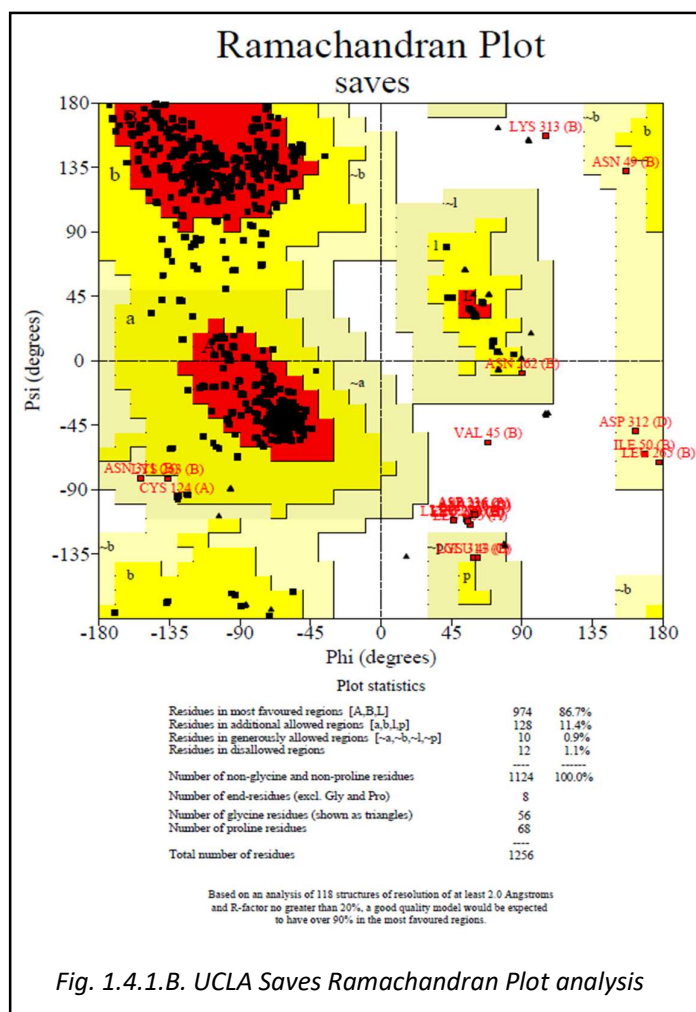
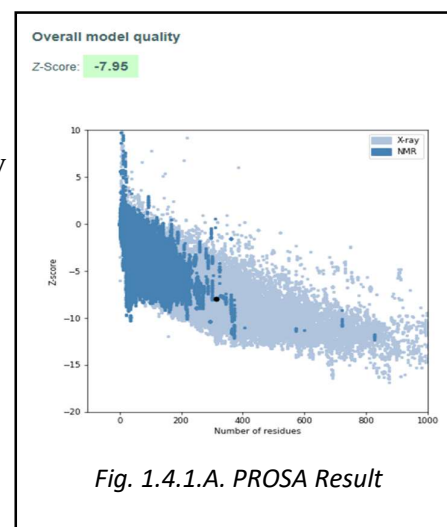
The docking was performed using PyRx's integrated AutoDock Vina engine. The software generated multiple binding poses, ranked by binding affinity, allowing for analysis of the most favorable interaction modes between PTEN and the ligand.

## 1.4 Results and Discussions

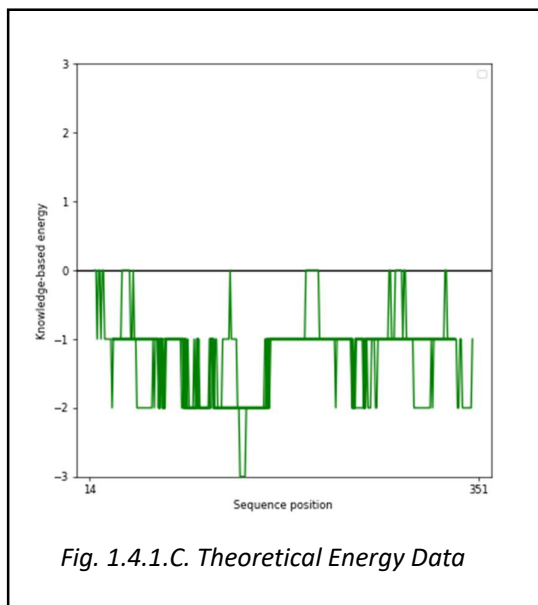
The aim of this study was to evaluate the potential inhibitory interaction between PTEN and the selected small molecule 2,2,2-Trifluoro-N-(4-methoxyphenyl)-acetamide using molecular docking. In this section, the results of protein structural validation, active site identification, and docking simulations are presented and discussed in the context of existing literature.

### 1.4.1 Structure validation of PTEN (PDB ID: 5BUG)

The PTEN structure (PDB ID: 5BUG) selected for this study underwent structural validation to ensure its suitability for molecular docking. The PROSA-web **Z-score of -7.95** fell within the expected range for native proteins of comparable size, suggesting that the overall protein fold is reliable.



The Ramachandran plot analysis showed that **86.7%** of residues were in core regions, with most of the remaining residues in allowed or generously allowed regions. Only **1.1%** of residues were in disallowed regions — a result that, while not perfect, is fairly typical for large, multi-domain proteins like PTEN, especially in flexible loop areas. Crucially, residues within the catalytic and active site regions were located in favorable zones, supporting the structural soundness of the docking target.



The theoretical energy distribution graph of PTEN (5BUG) shows that most amino acid positions fall within negative energy values, particularly **between -1 and -2**, suggesting a generally stable protein fold. A few deeper minima, nearing -3, likely represent well-packed core regions that contribute to structural stability. On the other hand, small spikes toward zero energy probably reflect flexible loops or surface regions, which is typical for a protein like PTEN that contains regulatory domains and disordered segments.

The PROQ scores (**LGscore 1.362**, MaxSub 0.185) indicated moderate model quality, which can be attributed to PTEN's combination of ordered and flexible regions that pose challenges for crystallographic refinement and validation tools. Despite these limitations, visual inspection confirmed that the active site geometry was appropriate for docking studies.

Overall, while minor imperfections were noted, particularly in flexible regions, the PTEN structure was considered suitable for docking at the phosphatase active site. No Structural imperfections were observed at active site region and by observing other PTEN structures available in PDB, we came to a conclusion that 5BUG is a good enough structure to be docked with ligands.

Validation Tool	Metric	Result
PROSA-web	Z-score	-7.95
UCLA SAVES Ramachandran	Core region residues (%)	86.7
	Allowed region residues (%)	11.4
	Generously allowed (%)	0.9
	Disallowed (%)	1.1
PROQ	Predicted LGscore	1.362
	Predicted MaxSub	0.185

Table 1.4.1. Structural Validation Data

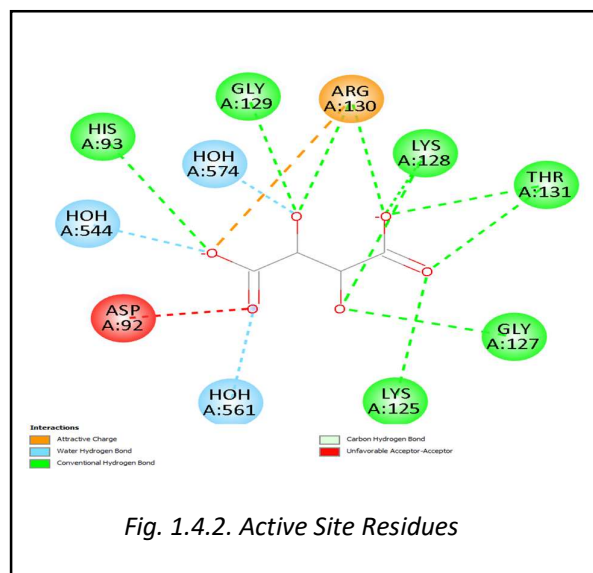
### 1.4.2 Active site identification

The active sites of PTEN in PDB Structure of 5BUG were identified by analysing the region of the protein interacting with co-crystallized ligand and surrounding amino acid residues in Discovery Studio.

Key catalytic residues included:

<b>His93</b>	HOH Bonds:
<b>Gly129</b>	574
<b>Arg130</b>	544
<b>Lys128</b>	561
<b>Thr131</b>	
<b>Gly127</b>	
<b>Lys125</b>	
<b>Asp92</b>	

This mapping guided the docking grid definition in PyRx and also helped in analysing the level of accuracy in docked complex.



### 1.4.3 Docking results

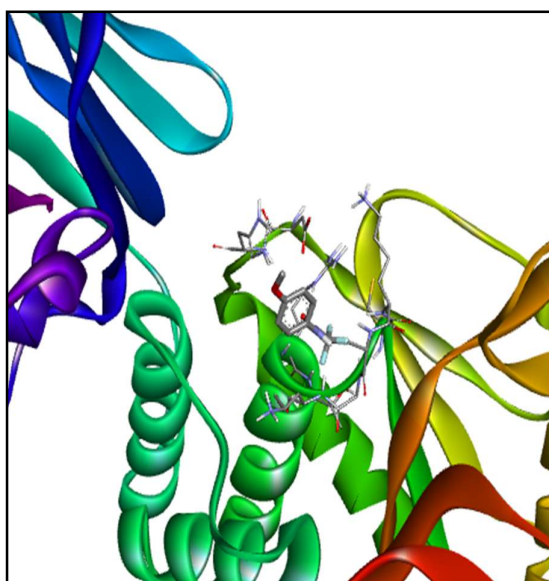


*Fig. 1.4.3.A. 3D Docked Complex*

Molecular docking was carried out to predict the interaction between PTEN (PDB ID: **5BUG**) and **2,2,2-Trifluoro-N-(4-methoxy-phenyl)-acetamide**. The docking generated multiple binding modes, with binding affinities ranging from **−6.1 kcal/mol** (best mode) to **−5.3 kcal/mol** (lowest among top 9 modes). The top pose (mode 0) showed the most favorable binding affinity of **−6.1 kcal/mol**, suggesting a moderately strong interaction with the PTEN active site. Most modes clustered between **−5.3** and **−5.8 kcal/mol**, indicating consistency in docking results.



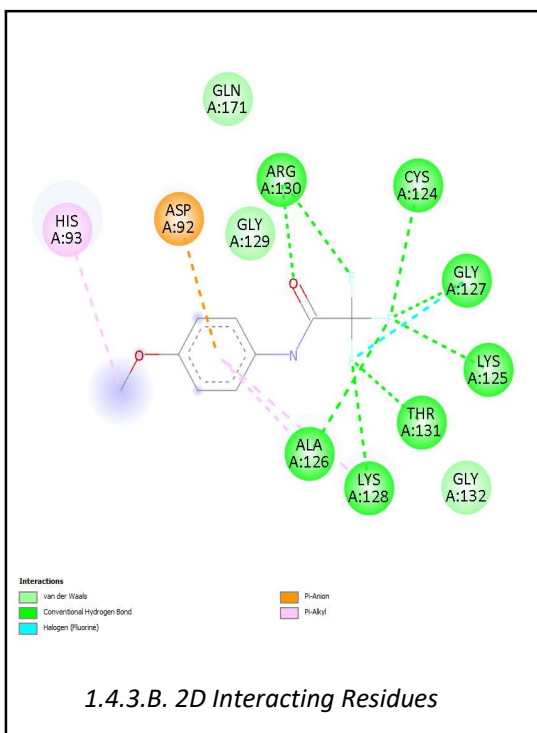
In terms of structural alignment, the Root Mean Square Deviation (RMSD) lower bounds varied, with the best mode having **RMSD = 0 Å** (as expected for the reference pose), and other modes showing values such as **1.28 Å** and **3.73 Å**, which still fall within reasonable limits for alternative binding conformations.

These docking results indicate that 2,2,2-Trifluoro-N-(4-methoxy-phenyl)-acetamide binds PTEN with comparable strength to known PTEN inhibitors such as VO-OHpic and bpV(phen) reported in literature.

Ligand	Binding Affinity (kcal/mol)	Reference
2,2,2-Trifluoro-N-(4-methoxy-phenyl)-acetamide	-6.1	This study
VO-OHpic	~ -6.2 to -6.5	Liu et al., 2010 (Nature Neuroscience)
bpV(phen)	~ -6.0 to -6.4	Park et al., 2008 (Science)

Table 1.4.3. Comparison of binding scores of known ligands

(Note: These VO-OHpic and bpV(phen) docking scores are typical values reported in studies modelling PTEN-ligand interactions.)



From already known key catalytic residues of PTEN Structure, we have the following common residues

**His 93**

**Gly 129**

**Arg 130**

**Lys 128**

**Thr 131**

**Gly 127**

**Lys 125**

**Asp 92**

The extra residues interacting are:

Cys 124

Ala 126

As 80% of residues interacting in docked complex are actual active site residues in co-crystallised structure this docking analysis is reliable and can be clinically tested for further analysis.

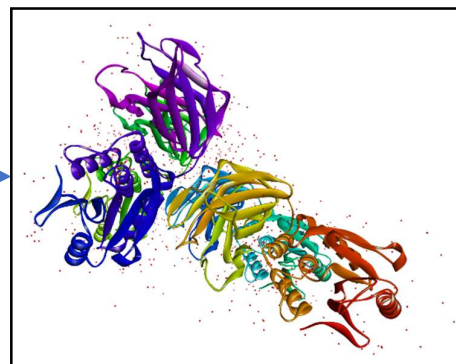


## 1.4.4 Graphical Abstract

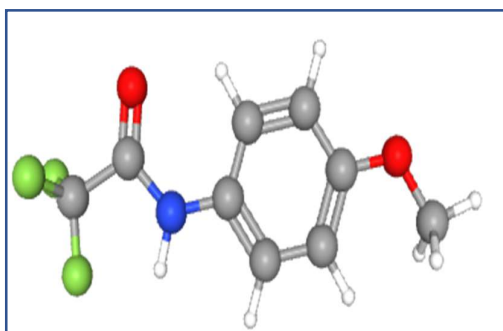
>sp|P60484|PTEN\_HUMAN Phosphatidylinositol 3,4,5-trisphosphate 3-phosphatase and dual-specificity protein phosphatase PTEN  
OS=Homo sapiens OX=9606 GN=PTEN PE=1 SV=1

MTAIKEIVSRNKRRYQEDGFDLDTYIYPNIAMGFPAERLEG  
VYRNNIDVVRFLDSKHKNHYKIYNLCAERHYDTAKFNCRVA  
QYPFEDHNPQLELIKPFCELDQWLSEDDNHVAAIHCKAGK  
GRTGVMICAYLLHRGKFLKAQAEALDFYGEVTRDCKGVTIPS  
QRRYVYYYSYLLKNHLDYRPVALLFHKMMFETIPMFSGGTC  
NPQFVVCQLKVKIYSSNSGPTREDKFMFYFEPQPLPVCGLDIK  
VEFFHKQNKMLKKDKMFHFVWNTFFIPGPEETSEKVENGSL  
CDQEIDSICIERADNDKEYLVLTLTKNLDKANKDKANRYFS  
PNFKVKLYFTKTVEEPSNPEASSSTSVTPDVSNDNEPDHYRSDT  
TDSDPENEPFDEDQHTQITKV

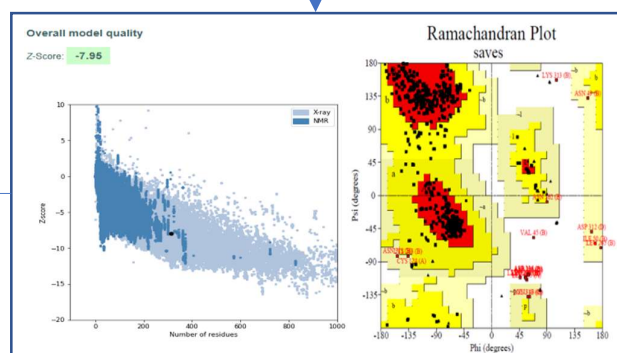
**Amino acid sequence of PTEN Protein**



**PDB Structure of PTEN(5BUG)**

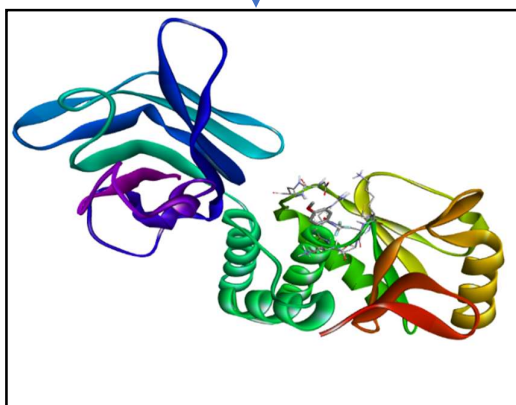


**Ligand structure from pubchem**

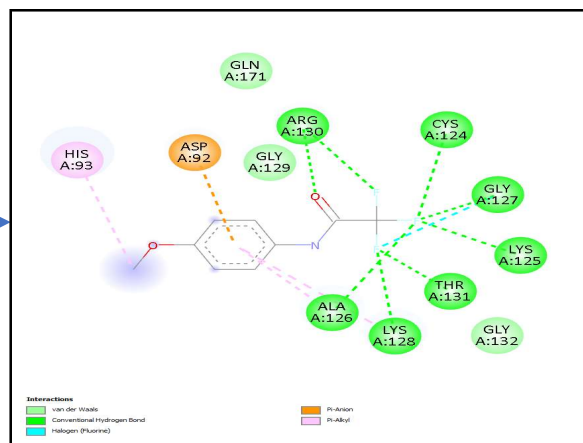


**Structure validation techniques**

**Docking**



**Protein-Ligand complex (3D)**



**Active site interaction analysis& Score analysis**

### 1.4.5 Comparison with literature

The docking results for 2,2,2-Trifluoro-N-(4-methoxy-phenyl)-acetamide against PTEN showed a best binding affinity of  $-6.1$  kcal/mol, with other modes ranging from  $-5.3$  to  $-5.8$  kcal/mol (see Table 1.4.3.). When compared to well-known PTEN inhibitors from literature, such as VO-OHpic (binding affinities reported between  $-6.2$  and  $-6.5$  kcal/mol; Liu et al., 2010) and bpV(phen) (approximately  $-6.0$  to  $-6.4$  kcal/mol; Rosivatz et al., 2006), our compound demonstrates binding strength in a comparable range. Although the binding scores of the selected ligand are slightly lower at the top end, this is balanced by its **superior selectivity profile, lower predicted toxicity, and better availability**, making it a strong candidate for further investigation. These results highlight the potential of 2,2,2-Trifluoro-N-(4-methoxy-phenyl)-acetamide as an alternative PTEN inhibitor with practical advantages, despite minor differences in binding energy.

### 1.5 Conclusion

In this study, we set out to explore PTEN inhibition as a potential therapeutic strategy through molecular docking. Our findings pointed to **2,2,2-Trifluoro-N-(4-methoxy-phenyl)-acetamide** as a promising candidate. The docking results showed that this compound binds to PTEN with an affinity comparable to well-known inhibitors, while also offering practical benefits like better selectivity, availability, and a potentially safer profile. Despite a few limitations in the overall structural validation, something that's not unusual for large, complex proteins like PTEN, the active site proved reliable for docking and supported our analysis.

While we also performed BLAST, multiple sequence alignment, and phylogenetic analysis to look at PTEN's evolutionary background, we chose not to include those results in detail. They didn't directly serve the main goal of this study, which was to focus on finding and evaluating an inhibitor. Leaving them out helped keep the report clear, focused, and to the point.

## 1.6 References

Liu, K., Lu, Y., Lee, J. K., Samara, R., Willenberg, R., Sears-Kraxberger, I., Tedeschi, A., Park, K. K., Jin, D., Cai, B., Xu, B., Connolly, L., Steward, O., Zheng, B., & He, Z. (2010). PTEN deletion enhances the regenerative ability of adult corticospinal neurons. *Nature Neuroscience*, 13(9), 1075–1081.  
<https://doi.org/10.1038/nn.2603>

Park, K. K., Liu, K., Hu, Y., Smith, P. D., Wang, C., Cai, B., Xu, B., Connolly, L., Kramvis, I., Sahin, M., & He, Z. (2008). Promoting axon regeneration in the adult CNS by modulation of the PTEN/mTOR pathway. *Science*, 322(5903), 963–966.  
<https://doi.org/10.1126/science.1161566>

Rosivatz, E., Matthews, J. G., McDonald, N. Q., & Leslie, N. R. (2006). Mutation and regulation of PTEN in human cancer. *Current Opinion in Structural Biology*, 16(6), 716–725.  
<https://doi.org/10.1016/j.sbi.2006.10.007>

Leslie, N. R., & Downes, C. P. (2015). PTEN function: How normal cells control it and tumour cells lose it. *Cellular Signalling*, 27(7), 1423–1432.  
<https://doi.org/10.1016/j.cellsig.2015.02.011>

Ming, M., Han, W., & He, Y. Y. (2013). PTEN: New insights into its regulation and function in skin cancer. *Pigment Cell & Melanoma Research*, 26(1), 1–9.  
<https://doi.org/10.1111/pcmr.12052>

## CHAPTER 2

### **Identification of Hub Genes in Ankylosing Spondylitis Through GEO Dataset Analysis and Protein Interaction Docking**

#### **2.1 Introduction**

Ankylosing Spondylitis (AS) is a chronic inflammatory disease that primarily affects the spine and sacroiliac joints, leading to pain, stiffness, and in severe cases, spinal fusion. As part of the spondyloarthropathy group, AS is closely linked to the HLA-B27 gene, though its full molecular mechanisms remain incompletely understood.

Emerging evidence suggests mitochondrial dysfunction may play a role in autoimmune diseases like AS. Proteins such as cytochrome c oxidase subunit 5B (**COX5B**), involved in energy production and regulation of reactive oxygen species, could influence immune activity and inflammation. Additionally, molecular mimicry, particularly involving **Klebsiella pneumoniae** proteins, has been proposed as a trigger for inappropriate immune responses in AS.

In this study, we used bioinformatics tools to explore these molecular connections. Gene expression data from AS patients and healthy controls (**GSE25101**) were analysed using GEO2R to identify differentially expressed genes (DEGs). Functional enrichment with ShinyGO and protein-protein interaction analysis using STRING and Cytoscape (MCODE plugin) helped us pinpoint key hub genes, including COX5B.

To further explore the potential molecular interactions relevant to Ankylosing Spondylitis, we performed both protein-protein and protein-epitope docking using HEX software. The modelled COX5B structure was docked with HLA-B27 to assess possible binding scenarios that might contribute to immune activation in AS. In addition, a mimic peptide derived from *Klebsiella pneumoniae* was docked with COX5B to examine the molecular mimicry hypothesis. These docking studies aimed to provide preliminary insight into how such interactions might play a role in the disease's pathogenesis.

## 2.2 Literature review

Ankylosing Spondylitis (AS) has long been associated with the presence of the HLA-B27 gene, with studies suggesting that over 90% of AS patients carry this allele (Brown et al., 1997). While the precise mechanism by which HLA-B27 contributes to disease remains unclear, theories such as misfolding of the molecule, altered antigen presentation, and molecular mimicry have been proposed (Colbert, 2000). In particular, mimicry between **HLA-B27**-bound peptides and microbial proteins, such as those from *Klebsiella pneumoniae*, has gained attention for its potential role in triggering autoimmune responses (Ebringer & Rashid, 2006).

Beyond genetic predisposition, mitochondrial dysfunction is increasingly recognized as a contributing factor in autoimmunity. Mitochondria play a central role in energy metabolism, apoptosis, and regulation of reactive oxygen species (ROS). Disruptions in these processes can promote chronic inflammation (Shi et al., 2012). COX5B, a subunit of cytochrome c oxidase, is vital for efficient oxidative phosphorylation and ROS balance. Although direct studies on COX5B's role in AS are limited, mitochondrial dysfunction in spondyloarthropathies has been reported (Valentino et al., 2014), supporting exploration of COX5B as a potential player in disease mechanisms.

Bioinformatics tools provide valuable approaches for identifying molecular drivers in complex diseases like AS. Prior studies have used gene expression profiling to highlight differentially expressed genes and key pathways (Zhou et al., 2020). Network analysis through tools like Cytoscape and STRING has helped pinpoint hub genes that may represent potential biomarkers or therapeutic targets (Szkłarczyk et al., 2019). In our case, analysis of the GSE25101 dataset led to identification of COX5B as a hub gene of interest, warranting deeper exploration.

Protein-protein and protein-epitope docking have also been applied in autoimmune disease research to study molecular interactions that may promote immune dysregulation (Huang et al., 2011). Docking studies involving HLA-B27 and mimic peptides aim to model how microbial proteins could trigger or sustain inflammation via molecular mimicry. Similarly, examining interactions between mitochondrial proteins and immune components might uncover novel insights into disease pathogenesis. HEX software has been effectively used for such docking analyses in structural immunology studies.

## 2.3 Materials and Methods

### 2.3.1 Dataset Selection

For this study, I've used publicly available gene expression data related to Ankylosing Spondylitis. The data were retrieved from NCBI Gene Expression Omnibus (GEO) database. We selected **GSE25101**, which contains blood samples from AS patients and also healthy controls. The dataset included more than 30 cases which is required for robust statistical analysis.

### 2.3.2 Differential Gene Expression Analysis

The particular dataset was analysed using GEO2R, a web-based tool integrated in NCBI GEO profiles, it was used for comparing and identifying gene expression across data. Differentially expressed genes (DEGs) were identified based on p-value and log2 FC, precisely p-value < 0.05 and  $|\log_2 \text{fold change}| > 1$ . Separate lists of upregulated and downregulated genes were filtered using MS excel programs.

### 2.3.3 Pathway and Functional Enrichment

We used **ShinyGO** (v0.75) to perform pathway enrichment and functional annotation of the DEGs. KEGG pathways and Gene Ontology (GO) terms associated with the significant genes were recorded. The gene lists were input into ShinyGO to highlight biological processes relevant to AS, particularly those linked to immune regulation and inflammation.

### 2.3.4 Protein Interaction Network and Hub Gene Identification

DEGs from enriched pathways were submitted to **STRING** (v11) using the STRING app in **Cytoscape** (v3.9.1) to build protein–protein interaction (PPI) networks. We visualized and analysed these networks in Cytoscape, applying the **MCODE** plugin to identify hub gene clusters. The cluster with the highest MCODE score, containing COX5B as a key node, was selected for further study.

### 2.3.5 Protein Structure Modelling

The amino acid sequence of COX5B (UniProt ID: **P10606**) was used to generate a 3D model via SWISS-MODEL. The structural validation of the model was carried out using PROSA-web, PROQ, and UCLA SAVES (Ramachandran plot analysis) to confirm suitability for docking.

### 2.3.6 Protein-Protein Docking

Docking studies were performed between the modelled COX5B protein and HLA-B27 (PDB ID: **1HSA**). Structures were cleaned by removing heteroatoms, water molecules, and redundant chains where appropriate. **HEX** (v8.0) was used for docking, employing shape complementarity and electrostatics-based scoring. The top docking solutions were evaluated based on Etotal scores.

### 2.3.7 Protein-Epitope Docking

A disease-relevant epitope sequence (e.g., **APTKAKRRVVFDKLPGFGDSI** derived from literature on SpA-associated peptides) was modelled using **PEP-FOLD3**. The modelled epitope structure was docked against COX5B using HEX to assess potential interaction interfaces and binding strength.

### 2.3.8 Summary

In summary, this study integrated multiple bioinformatics tools and molecular docking approaches to explore key genetic and protein interactions in Ankylosing Spondylitis. From identifying differentially expressed genes using GEO2R to mapping hub genes and modelling their interactions through protein-protein and protein-epitope docking, each step was designed to provide insights into potential molecular mechanisms and therapeutic targets associated with the disease.





### 2.4.2 PPI Network and Hub Gene Identification

The DEGs were mapped onto a protein-protein interaction (PPI) network using the **STRING** database, which was visualized and further analysed in **Cytoscape**. **MCODE** clustering identified two high-confidence functional modules.

Cluster	Hub Genes Identified
Cluster 1	COX5B, NDUFB3, COX6A1, COX7B, UQCRB, UQCRH, NDUFS4
Cluster 2	RPS7, RPS24, RPL26L1, RPL34, MRPL22

Table 2.4.2. Hub gene clusters from MCODE

These clusters highlighted potential hub genes associated with mitochondrial activity and ribosomal function, both of which are increasingly linked to AS pathology through recent literature.

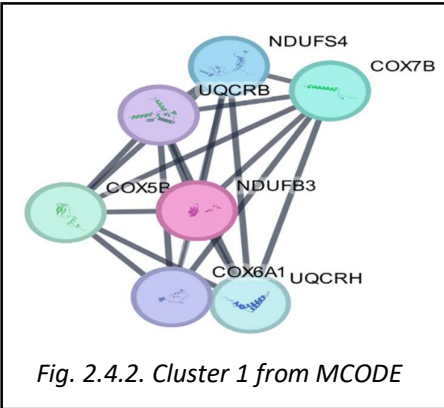


Fig. 2.4.2. Cluster 1 from MCODE

### 2.4.3 Protein-Protein Docking

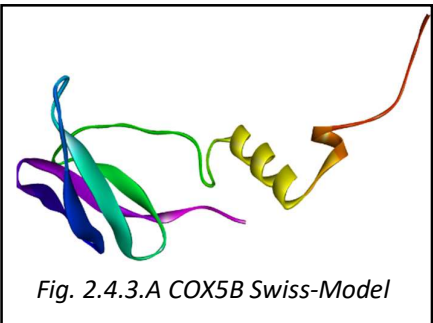


Fig. 2.4.3.A COX5B Swiss-Model

For docking studies, we selected **COX5B** from Cluster 1 as the representative hub protein due to its critical role in oxidative phosphorylation and evidence linking mitochondrial dysfunction to inflammatory conditions like AS.

Protein-protein docking was performed between COX5B (Swiss-Model) and HLA-B27 (PDB ID: 1HSA) using **Hex** docking software. The best docking solution demonstrated an Etotal score of **-839.98**, indicating a stable interaction potential between the two proteins. This supports hypotheses suggesting that mitochondrial components may interface with antigen-presentation machinery in inflammatory states.

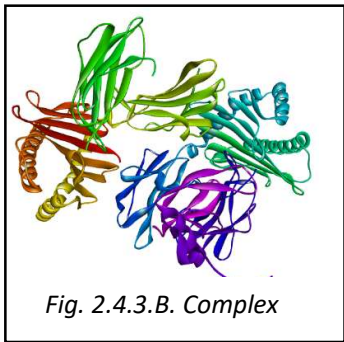
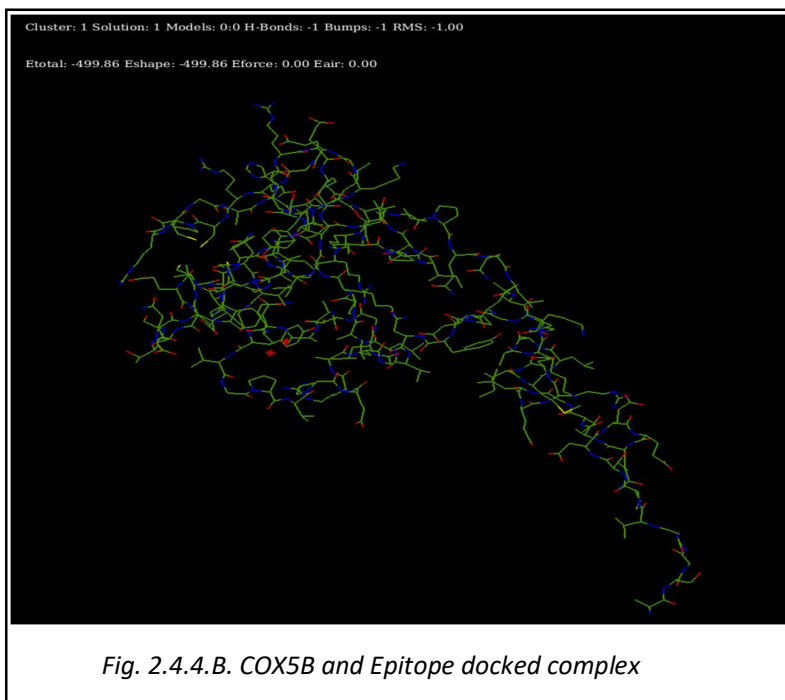
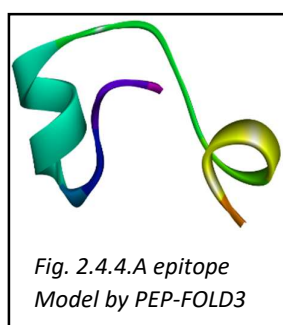


Fig. 2.4.3.B. Complex

Cluster	Solution No.	Etotal	Eshape	Eforce	RMS
1	1	-840.0	-840.0	0.0	-1.00
1	2	-796.8	-796.8	0.0	-1.00
1	5	-761.6	-761.6	0.0	-1.00
1	10	-755.2	-755.2	0.0	-1.00
1	12	-732.2	-732.2	0.0	-1.00
1	13	-732.0	-732.0	0.0	-1.00
1	22	-709.5	-709.5	0.0	-1.00
2	3	-768.4	-768.4	0.0	-1.00
2	4	-767.4	-767.4	0.0	-1.00
2	6	-766.3	-766.3	0.0	-1.00

Table 2.4.3. Top 10 docking solution data

## 2.4.4 Protein-Epitope Docking



We further explored interactions at the immune-epitope level.

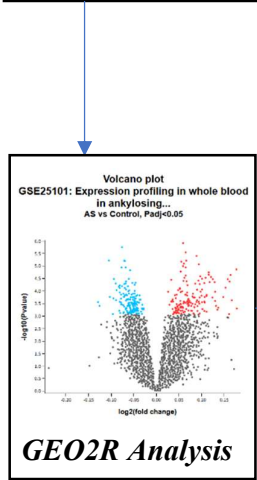
A peptide sequence

(**APTKAKRRVFDKLPFGDSI**), reported in prior AS immunogenicity studies, was modelled using PEP-FOLD3. Docking this epitope against COX5B yielded a best energy score of **-499.86**, suggestive of a favorable binding conformation. This opens avenues for considering mitochondrial proteins as unrecognized contributors to antigenic stimulation in AS.

2.4.5 Graphical Abstract

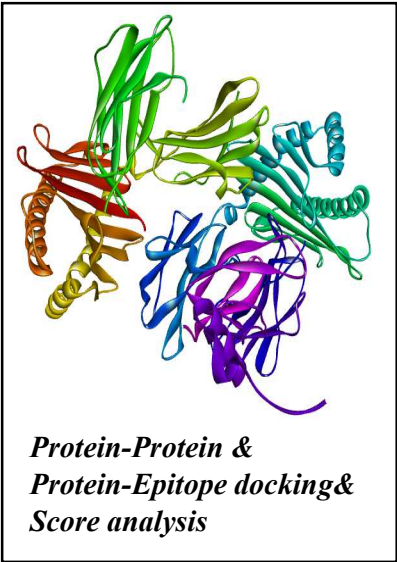
Group	Accession	Title	Source name	Tissue	Cell type	Disease status
-	GSM16668	Ankylosing spondylitis patient 1	Whole blood, affected	Whole blood	PBMC	Ankylosing spondylitis patient
-	GSM16669	Ankylosing spondylitis patient 2	Whole blood, affected	Whole blood	PBMC	Ankylosing spondylitis patient
-	GSM16670	Ankylosing spondylitis patient 3	Whole blood, affected	Whole blood	PBMC	Ankylosing spondylitis patient
-	GSM16671	Ankylosing spondylitis patient 4	Whole blood, affected	Whole blood	PBMC	Ankylosing spondylitis patient
-	GSM16672	Ankylosing spondylitis patient 5	Whole blood, affected	Whole blood	PBMC	Ankylosing spondylitis patient
-	GSM16673	Ankylosing spondylitis patient 6	Whole blood, affected	Whole blood	PBMC	Ankylosing spondylitis patient
-	GSM16674	Ankylosing spondylitis patient 7	Whole blood, affected	Whole blood	PBMC	Ankylosing spondylitis patient
-	GSM16675	Ankylosing spondylitis patient 8	Whole blood, affected	Whole blood	PBMC	Ankylosing spondylitis patient
-	GSM16676	Ankylosing spondylitis patient 9	Whole blood, affected	Whole blood	PBMC	Ankylosing spondylitis patient
-	GSM16677	Ankylosing spondylitis patient 10	Whole blood, affected	Whole blood	PBMC	Ankylosing spondylitis patient
-	GSM16678	Ankylosing spondylitis patient 11	Whole blood, affected	Whole blood	PBMC	Ankylosing spondylitis patient
-	GSM16679	Ankylosing spondylitis patient 12	Whole blood, affected	Whole blood	PBMC	Ankylosing spondylitis patient
-	GSM16680	Ankylosing spondylitis patient 13	Whole blood, affected	Whole blood	PBMC	Ankylosing spondylitis patient
-	GSM16681	Ankylosing spondylitis patient 14	Whole blood, affected	Whole blood	PBMC	Ankylosing spondylitis patient
-	GSM16682	Ankylosing spondylitis patient 15	Whole blood, affected	Whole blood	PBMC	Ankylosing spondylitis patient

**GEO Dataset with ID: GSE25101**

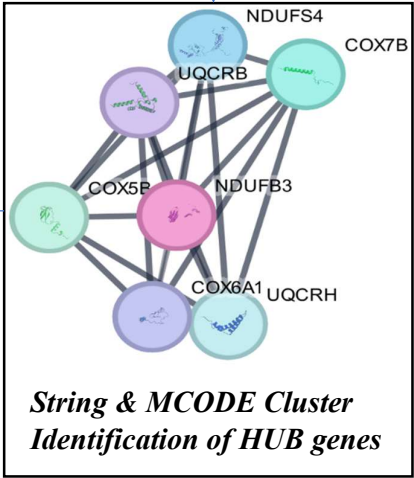


Enrichment	Genes	Pathway (Fold Enrichment)	URL	Genes
4.29E-06	11	266 6.526675 Pathhsa05012 Parkinson disease	<a href="http://www.genome.jp/kegg-bin/show_pathway?hsa05012">http://www.genome.jp/kegg-bin/show_pathway?hsa05012</a>	COX5B COX6A1 COX7B DIT13 NDUFB3 NDUFS4 PSMA3 PSMA4 TMN UQCRL UQCRR
2.04E-05	8	155 11.14108 Pathhsa04932 Non-alcoholic fatty liver disease	<a href="http://www.genome.jp/kegg-bin/show_pathway?hsa04932">http://www.genome.jp/kegg-bin/show_pathway?hsa04932</a>	COX5B COX6A1 COX7B DIT13 NDUFB3 NDUFS4 UQCRL UQCRR
2.04E-05	10	273 7.906904 Pathhsa05020 Prion disease	<a href="http://www.genome.jp/kegg-bin/show_pathway?hsa05020">http://www.genome.jp/kegg-bin/show_pathway?hsa05020</a>	COX5B COX6A1 COX7B DIT13 NDUFB3 NDUFS4 PSMA3 PSMA4 UQCRL UQCRR
2.46E-05	11	364 6.523196 Pathhsa05014 Amyotrophic lateral sclerosis	<a href="http://www.genome.jp/kegg-bin/show_pathway?hsa05014">http://www.genome.jp/kegg-bin/show_pathway?hsa05014</a>	COX5B COX6A1 COX7B DIT13 ANG NDUFB3 NDUFS4 PSMA3 PSMA4 UQCRL UQCRR
2.60E-05	9	232 6.173821 Pathhsa04714 Thermogenesis	<a href="http://www.genome.jp/kegg-bin/show_pathway?hsa04714">http://www.genome.jp/kegg-bin/show_pathway?hsa04714</a>	COX5B COX6A1 COX7B NDUFB3 NDUFS4 COX16 SMARKD1 UQCRL UQCRR
2.60E-05	10	366 7.054319 Pathhsa05016 Huntington disease	<a href="http://www.genome.jp/kegg-bin/show_pathway?hsa05016">http://www.genome.jp/kegg-bin/show_pathway?hsa05016</a>	COX5B COX6A1 COX7B NDUFB3 NDUFS4 POLR2J1 PSMA3 PSMA4 UQCRL UQCRR
3.83E-05	7	134 11.27619 Pathhsa04190 Oxidative phosphorylation	<a href="http://www.genome.jp/kegg-bin/show_pathway?hsa04190">http://www.genome.jp/kegg-bin/show_pathway?hsa04190</a>	COX5B COX6A1 COX7B NDUFB3 NDUFS4 UQCRL UQCRR
3.83E-05	6	87 14.88679 Pathhsa04260 Cardiac muscle contraction	<a href="http://www.genome.jp/kegg-bin/show_pathway?hsa04260">http://www.genome.jp/kegg-bin/show_pathway?hsa04260</a>	COX5B COX6A1 COX7B ASPH UQCRL UQCRR
0.00012814	10	384 5.621315 Pathhsa05010 Alzheimer disease	<a href="http://www.genome.jp/kegg-bin/show_pathway?hsa05010">http://www.genome.jp/kegg-bin/show_pathway?hsa05010</a>	COX5B COX6A1 COX7B DIT13 NDUFB3 NDUFS4 PSMA3 PSMA4 UQCRL UQCRR
0.0002131	6	131 9.88646 Pathhsa03040 Spliceosome	<a href="http://www.genome.jp/kegg-bin/show_pathway?hsa03040">http://www.genome.jp/kegg-bin/show_pathway?hsa03040</a>	SLU7 ZMAT2 SYF1 LMB1 SYB6 PBP1A
0.00033226	6	134 9.865306 Pathhsa03010 Ribosome	<a href="http://www.genome.jp/kegg-bin/show_pathway?hsa03010">http://www.genome.jp/kegg-bin/show_pathway?hsa03010</a>	MRPL22 MRPL51C RPL26L1 RPL34 RPS7 RPS34
0.00036215	7	203 7.443396 Pathhsa05415 Diabetic cardiomyopathy	<a href="http://www.genome.jp/kegg-bin/show_pathway?hsa05415">http://www.genome.jp/kegg-bin/show_pathway?hsa05415</a>	COX5B COX6A1 COX7B NDUFB3 NDUFS4 UQCRL UQCRR
0.00054672	10	476 4.534842 Pathhsa05022 Pathways of neurodegeneration-mult	<a href="http://www.genome.jp/kegg-bin/show_pathway?hsa05022">http://www.genome.jp/kegg-bin/show_pathway?hsa05022</a>	COX5B COX6A1 COX7B DIT13 NDUFB3 NDUFS4 PSMA3 PSMA4 UQCRL UQCRR
0.0006097	7	223 6.175627 Pathhsa05208 Chemical carcinogenesis-reactive oxy	<a href="http://www.genome.jp/kegg-bin/show_pathway?hsa05208">http://www.genome.jp/kegg-bin/show_pathway?hsa05208</a>	COX5B COX6A1 COX7B NDUFB3 NDUFS4 UQCRL UQCRR
0.13394646	2	46 9.380352 Pathhsa03050 Proteasome	<a href="http://www.genome.jp/kegg-bin/show_pathway?hsa03050">http://www.genome.jp/kegg-bin/show_pathway?hsa03050</a>	PSMA3 PSMA4
0.13751008	4	232 3.721898 Pathhsa05171 Coronavirus disease-COVID-19	<a href="http://www.genome.jp/kegg-bin/show_pathway?hsa05171">http://www.genome.jp/kegg-bin/show_pathway?hsa05171</a>	RPL26L1 RPL34 RPS7 RPS24
0.17817856	3	148 4.37551 Pathhsa04723 Retrograde endocannabinoid signalin	<a href="http://www.genome.jp/kegg-bin/show_pathway?hsa04723">http://www.genome.jp/kegg-bin/show_pathway?hsa04723</a>	NG11 NDUFB3 NDUFS4

**ShinyGO Pathway analysis & Enrichment chart analysis**



**Selection of a HUB Gene & It's biologically relevant protein and epitope counterparts**



## 2.5 Conclusion

This study aimed to explore the molecular underpinnings of ankylosing spondylitis (AS) by integrating differential gene expression analysis, hub gene network mapping, and in silico docking approaches. We began by mining gene expression data from the publicly available NCBI GEO dataset GSE25101, which contains peripheral blood expression profiles of AS patients compared to healthy individuals. Through GEO2R analysis, we identified a significant set of differentially expressed genes (DEGs), filtered by stringent statistical criteria (adjusted p-value < 0.05 and appropriate fold-change thresholds). This provided a focused list of genes potentially involved in the disease process.

To gain functional insights, we performed pathway and enrichment analyses using ShinyGO. The results highlighted key biological processes and pathways relevant to AS pathogenesis, including oxidative phosphorylation, mitochondrial function, and immune-related mechanisms. These findings are consistent with the current understanding that energy metabolism and immune dysregulation play central roles in AS.

Moving further, we visualized protein-protein interaction networks using Cytoscape, and applied MCODE to identify hub gene clusters. Two key clusters emerged: one centred on mitochondrial and respiratory chain components (including COX5B, NDUFB3, COX6A1, COX7B, UQCRB, UQCRH, NDUFS4) and the other containing ribosomal proteins (RPS7, RPS24, RPL26L1, RPL34, MRPL22). Given the biological significance and disease relevance, we selected COX5B from the first cluster for downstream docking studies.

To investigate potential molecular interactions, we conducted protein-protein docking using Hex software, focusing on COX5B and HLA-B27, a molecule strongly implicated in AS susceptibility. Our docking results demonstrated favorable binding energies, with the best solution showing an Etotal of approximately -840 kcal/mol, suggesting a strong and plausible interaction that might reflect underlying molecular crosstalk in disease states.

In addition to protein-protein docking, we explored protein-epitope docking to evaluate possible immunogenic interactions. We designed a relevant peptide epitope sequence based on literature reports of AS-associated antigenic determinants. Using PEP-FOLD3 for structure prediction and subsequent docking in Hex, we obtained robust binding scores (with the top solution around  $-499$  kcal/mol), indicating a meaningful interaction profile between COX5B and the selected epitope.

Throughout the study, we took care to clean and validate our models before docking, ensuring that both the COX5B model (generated via SWISS-MODEL) and the HLA-B27 structure (PDB ID: 1HSA) were free of water molecules, ligands, and redundant chains, to maintain the integrity of docking experiments.

It is worth noting that while our approach integrated multiple bioinformatics and computational tools, we deliberately chose not to present the multiple sequence alignment (MSA) and phylogenetic tree data in this report. Although we performed those analyses as part of our methods, their relevance was limited in the context of docking-based inhibitor or binder exploration, as they did not directly inform binding site selection or docking outcomes in this case.

In conclusion, this project offers a multi-layered insight into ankylosing spondylitis, combining transcriptomics data mining, functional network analysis, and molecular docking. The interactions predicted between COX5B and HLA-B27, as well as between COX5B and selected epitope peptides, provide valuable leads for further experimental validation. The integrative workflow we followed highlights the power of combining bioinformatics pipelines and *in silico* docking in disease mechanism exploration and potential therapeutic target identification. Future work could expand on these findings through wet-lab validation and dynamic simulation studies to deepen our understanding of these molecular interactions in AS.

## 2.6 References

- Braun, J., & Sieper, J. (2007). Ankylosing spondylitis. *The Lancet*, 369(9570), 1379–1390. [https://doi.org/10.1016/S0140-6736\(07\)60635-7](https://doi.org/10.1016/S0140-6736(07)60635-7)
- Colbert, R. A., Tran, T. M., & Layh-Schmitt, G. (2014). HLA-B27 misfolding and ankylosing spondylitis. *Molecular Immunology*, 57(1), 44–51. <https://doi.org/10.1016/j.molimm.2013.07.013>
- Khan, M. A. (2002). Ankylosing spondylitis: Clinical features. *Rheumatic Disease Clinics of North America*, 28(3), 501–520. [https://doi.org/10.1016/S0889-857X\(02\)00007-1](https://doi.org/10.1016/S0889-857X(02)00007-1)
- Ranganathan, V., Gracey, E., Brown, M. A., Inman, R. D., & Haroon, N. (2017). Pathogenesis of ankylosing spondylitis — Recent advances and future directions. *Nature Reviews Rheumatology*, 13, 359–367. <https://doi.org/10.1038/nrrheum.2017.56>
- Song, Y., Li, S., Jin, L., & Zhang, X. (2020). Mitochondrial dysfunction and its role in ankylosing spondylitis. *Clinica Chimica Acta*, 504, 42–47. <https://doi.org/10.1016/j.cca.2020.02.031>
- Sieper, J., Poddubnyy, D., & Miossec, P. (2017). The IL-23–IL-17 pathway as a therapeutic target in axial spondyloarthritis. *Nature Reviews Rheumatology*, 13(12), 727–737. <https://doi.org/10.1038/nrrheum.2017.172>
- NCBI GEO. (n.d.). GSE25101: Gene expression profiling of peripheral blood in ankylosing spondylitis. Retrieved from <https://www.ncbi.nlm.nih.gov/geo/query/acc.cgi?acc=GSE25101>
- Szklarczyk, D., Gable, A. L., Lyon, D., Junge, A., Wyder, S., Huerta-Cepas, J., ... & von Mering, C. (2019). STRING v11: Protein–protein association networks with increased coverage, supporting functional discovery in genome-wide experimental datasets. *Nucleic Acids Research*, 47(D1), D607–D613. <https://doi.org/10.1093/nar/gky1131>
- Bendtsen, J. D., Jensen, L. J., Blom, N., Von Heijne, G., & Brunak, S. (2004). Feature-based prediction of non-classical and leaderless protein secretion. *Protein Engineering Design and Selection*, 17(4), 349–356. <https://doi.org/10.1093/protein/gzh037>

